Hot-melt extrusion process impact on polymer choice of Glyburide solid dispersions: The effect of wettability and dissolution

Maen Alshafiee, Mohammad K. Aljammal, Daniel Markl, Adam Ward, Karl Walton, Liam Blunt, Sachin Korde, Sudhir K. Pagire, Adrian L. Kelly, Anant Paradkar, Barbara R. Conway, Kofi Asare-Addo

PII: S0378-5173(19)30073-0
DOI: https://doi.org/10.1016/j.ijpharm.2019.01.038
Reference: IJP 18100

To appear in: *International Journal of Pharmaceutics*

Received Date: 6 December 2018
Revised Date: 21 January 2019
Accepted Date: 23 January 2019

Please cite this article as: M. Alshafiee, M.K. Aljammal, D. Markl, A. Ward, K. Walton, L. Blunt, S. Korde, S.K. Pagire, A.L. Kelly, A. Paradkar, B.R. Conway, K. Asare-Addo, Hot-melt extrusion process impact on polymer choice of Glyburide solid dispersions: The effect of wettability and dissolution, *International Journal of Pharmaceutics* (2019), doi: https://doi.org/10.1016/j.ijpharm.2019.01.038

Hot-melt extrusion process impact on polymer choice of Glyburide solid dispersions: The effect of wettability and dissolution

Maen Alshafiee[a], Mohammad K. Aljammal[a], Daniel Markl[b], Adam Ward[a], Karl Walton[c], Liam Blunt[c], Sachin Korde[d], Sudhir K. Pagire[d], Adrian L. Kelly[d, e], Anant Paradkar[d], Barbara R. Conway[a], Kofi Asare-Addo[a] *

[a] Department of Pharmacy, University of Huddersfield, Huddersfield, HD1 3DH, UK

[b] Strathclyde Institute of Pharmacy and Biomedical Sciences, University of Strathclyde, 161 Cathedral Street, G4 0RE Glasgow, UK

[c] EPSRC Future Metrology Hub, University of Huddersfield, Huddersfield, HD1 3DH, UK

[d] Centre for Pharmaceutical Engineering Science, University of Bradford, Bradford, West Yorkshire, UK

[e] IRC in Polymer Science and Technology, University of Bradford, Bradford, West Yorkshire, UK

*Corresponding author (Kofi Asare-Addo)

e-mail: k.asare-addo@hud.ac.uk

Tel: +44 1484 472360

Fax: +44 1484 472182

Submission: International Journal of Pharmaceutics

Abstract:

The aim of this study was to evaluate the choice of polymer and polymer level on the performance of the microstructure and wettability of hot-melt extruded solid dispersion of Glyburide (Gly) as a model drug. The produced solid dispersion were characterised using scanning electron microscopy (SEM), image analysis using a focus variation instrument (FVI), differential scanning calorimetry (DSC), X-ray powder diffraction (XRPD), X-ray microtomography (XμT), dynamic contact angle measurement and dissolution analysis using biorelevant dissolution media (FASSIF). SEM and focus variation analysis showed that the microstructure and surface morphology was significantly different between samples produced. This was confirmed by further analysis using XμT which showed an increase in polymer content brought about a decrease in porosity of the hot-melt extruded dispersions. DSC suggested complete amorphorisation of Gly whereas XRPD suggested incomplete amorphorisation. The static and dynamic contact angle measurement correlated with the dissolution studies using FASSIF media indicating that the initial liquid imbibition process as captured by the dynamic contact angle directly affects the dissolution performance.

Keywords: solid dispersion; glyburide; hot-melt extrusion; contact angle, Soluplus®; Kollidon® VA64

Abbreviations: Gly, glibenclamide or glyburide; DSC, differential scanning calorimetry; XRPD, x-ray powder diffraction; API, active pharmaceutical ingredient; BCS, biopharmaceutical classification system; SOL, Soluplus®; XμT, x-ray microtomography; FASSIF, fasted simulated intestinal fluid; ASD, amorphous solid dispersions; Kollidon® VA64 or PVP VA64, polyvinylpyrrolidone-vinyl acetate copolymer; DE, dissolution

efficiency; MDT, mean dissolution time; FVI, focus variation instrument; SEM, scanning electron microscopy; HME, hot-melt extrusion

1. Introduction:

The utilising of innovative combinatorial chemistry and high-throughput screening tools in drug discovery has led to more active pharmaceutical ingredients with poorly soluble properties reaching clinical stages of drug development processes. It is estimated that two out of five pharmaceutical compounds in the US market are considered poorly soluble (Fahr and Liu, 2007). Poorly soluble drugs are very challenging during pharmaceutical development as solubility, and further dissolution tends to be the rate-limiting step for these compounds entering the systemic circulations and giving the desired therapeutic response (Adebisi et al., 2016; Conway and Asare-Addo 2016). To overcome this challenge, several techniques are used. These techniques can be classified into two main categories (Savjani et al., 2012). I: physical modification such as particle size reduction, optimisation of microstructure, supercritical fluids or crystal habit (polymorphs and amorphous forms) II: Chemical modification such as salt formation and co-crystals., use of buffers or novel excipients (Adebisi et al., 2016; Al-Hamidi et al., 2015, 2013, 2010a, 2010b; Asare-Addo et al., 2018; Guillory, 2003; He et al., 2017; Nokhodchi et al., 2017; Rabinow, 2004; Ramirez et al., 2017; Stahl and Wermuth, 2018; Šupuk et al., 2013)

Each technique has its drawbacks. For example, the enhancement of solubility of a neutral, weakly acidic or weakly basic drug using salt formation is not always feasible. Reducing the size can also be limited as generating very fine particles can pose safety issues during handling (Vasconcelos et al., 2007; Serajuddin, 1999). One of the attractive routes to overcoming these problems is by manufacturing amorphous solid dispersions (ASD). ASD

systems are composed of amorphous drug stabilised by the presence of a polymer (Newman et al., 2015). Solid dispersions can be manufactured by either solvent evaporation techniques or melting methods. In the solvent evaporation technique the drug and polymer are dissolved in a solvent followed by the evaporation of the solvent using spray drying (Ali and Lamprecht 2017; Sawicki et al., 2016; Paudel et al., 2013) or freeze drying methods (Pas et al., 2018; Lian et al., 2014; Betageri and Makarla, 1995). Melting methods, especially hot-melt extrusion (HME) have many advantages including scalability, being a solvent and dust free method and has industrial applicability (Paudel et al., 2013). The drug-polymer is blended then fed through a hopper to a heated barrel of a twin screw extruder. In the extruder, the drug-polymer blend experiences very high shear and temperature which leads to the formation of a homogenous dispersion of the drug into the polymer matrix. The formed solid dispersion is then pushed through the die to get the solid dispersion threads which are then subjected to pelletisation and the pellets collected as a finished product. The physical properties and ultimately the performance of pellets can be controlled by either changing the processing parameters such as temperature, speed or twin-screw configuration or using different polymers (Van den Mooter, 2012).

Polyethyleneglycol–polyvinyl caprolactam–polyvinyl acetate grafted copolymer (PEG6000/vinylcaprolactam/vinyl acetate copolymer, Soluplus®, BASF, Germany) (Figure 1) is a promising polymer that has attracted a lot of attention over the last decade. Soluplus® possesses the advantages of improving both the process (Djuris et al., 2013) and the dissolution rate of poorly soluble drugs (Nagy et al., 2012). The addition of PEG 6000 and the low glass transition temperature enhances the processability and eliminates the **need** of a plasticiser. Soluplus® also improves the dissolution rates of poorly soluble drugs by forming a solid solution with the drug. Kollidon® VA64 or PVP VA64 (polyvinylpyrrolidone-vinyl acetate copolymer) (Figure 1) is another polymer which has been demonstrated to enhance

the dissolution rate of poorly soluble drugs (Ponnammal et al., 2018). PVP VA64 works by solubilising poorly soluble drugs and ultimately improving the dissolution rate. An enhancement in mechanical properties and the production of flexible extruded pellets has been reported for the use of PVP VA64 (Solanki et al., 2018). Both polymers are considered as safe excipients and easy to handle with good flowability properties (Djuris et al., 2013; Nagy et al., 2012).

Glyburide (Gly), used as a model drug, is an example of a poorly soluble weak acidic drug (Figure 1) with an estimated pKa of 5.3 (Löbenberg et al., 2000). The acidic properties of the drug and its pKa value suggests that the drug will be favourably absorbed in the upper intestine. Wei *et al* studied the solubility of Gly in biorelevant dissolution media and found that the solubility of Gly in biorelevant media increased as pH increased. FASSIF media at pH 7.4 had the highest solubility (Wei and Löbenberg, 2006). The objectives of this research was to prepare and characterise solid dispersion of Gly using Soluplus® (Sol) and PVP VA64 at two different polymer levels. It was therefore the aim of the authors to characterise the surface of the pellets using a focus variation instrument and to determine the effect polymer type and polymer level on wettability. The authors also investigated a correlation of the wettability of the solid dispersions (polymer level and type) with the performance of dissolution as to the best of our knowledge, there are no research articles that have studied this.

2. Materials and Methods

2.1. Materials

Poly (N-vinyl caprolactam)–poly (vinyl acetate)–poly (ethylene glycol) (57:30:13), under the trade name Soluplus® and polyvinylpyrrolidone-vinyl acetate copolymers branded as Kollidon® VA 64 were kind gifts from BASF (Germany). Gly was purchased from

Kemprotec (Cumbria, U.K.). FASSIF (fasted simulated intestinal fluid) powder was purchased from Biorelevant Ltd (Surrey, United Kingdom). PEG4000 was purchased from Sigma Aldrich (UK). Monobasic potassium phosphate, sodium hydroxide, ammonium acetate, acetic acid and acetonitrile were all purchased from Sigma Aldrich, UK. All materials were of analytical grade and used as obtained.

2.2. Preparation of hot-melt extruded (HME) solid dispersions

A 16 mm twin screw extruder (Pharmalab, Thermo Scientific, UK) was used to carry out the extrusion work. Gly and either PVP VA64 or Soluplus® at two different ratios (1:1 and 1:2) were mixed using a T2F Turbula Blender System (Willy A Bachofen AG) for 10 min in order to ensure uniformity of powder mixing. PEG 4000 was added to the PVP VA64 samples as a plasticiser and to improve the process of extrusion. Each powder mixture was then extruded using the hot-melt extruder. A maximum barrel temperature of 175 ^{o}C was used to ensure that the Gly was completely melted (melting point of Gly is 175 ^{o}C) (Betageri and Makarla, 1996) (**The configuration for the HME was a mixture of conveying and kneading elements with a stagger angle of 60 degrees for the kneading elements. The screw rotation speed was set at 100 rpm for all four sample batches. The temperatures of the nine heated barrel and die zones were set as shown in supplementary materials Table S1. The feeding rate of the powder was set at 5 g/min**). **Care was taken to ensure the degradation temperature of Gly which has been reported to range between 195 - 200 ^{o}C (Wei et al., 2008) was not reached by reading the actual temperature recorded during the HME process also.** The produced pellets were separated into two sub samples: the first samples were characterised as received from the HME process using SEM, a focus variation instrument and X-ray computed microtomography (XμT) to get an insight into the microstructure and its potential impact on dissolution. The second sample (pellets) were

further milled **using a mortar and pestle** and sieved to 250 µm undersize (to ensure the same size fractions were used) for all the samples **(all the milled samples were further analysed using a Laser diffraction instrument (Sympatec, UK) to further confirm the particle size distribution)** and characterised using DSC and XRPD to check the changes in the crystallinity of Gly. The latter samples were used in the dissolution testing and labelled as samples A-D (Sample A is 1:1 Gly:Sol, Sample B is 1:2 Gly:Sol, Sample C is 1:1 Gly:PVP VA 64 and Sample D is 1:2 Gly:PVP VA 64) and their corresponding physical mixtures labelled as samples PMA-PMD. **All samples were stored in a desiccator prior to use to decrease the potential effect of hygroscopicity.**

2.2.2 Content uniformity of Gly in milled and sieved samples

50 mg of the milled and sieved samples A-D were dissolved each in 50 mL acetonitrile and an assay was performed to determine the Gly content using the HPLC method as explained in section 2.6.3. The results from the assay were further used to determine the amount of powder needed to fill the gelatine capsules size 3 to ensure the same amount of Gly was present in each capsule.

2.3. Solid State characterisation:

2.3.1. Scanning electron microscopy (SEM) and image analysis using a focus variation instrument

A scanning electron microscope (Jeol JSM-6060CV SEM) operating at 10 kV was used to generate electron micrographs images. Pellets (Samples A-D) were cross-sectioned and mounted onto a metal stub using a double-sided adhesive tape. Samples were then sputter-coated with gold for 60 s using a Quorum SC7620. Micrographs with different

magnifications were taken to aid an understanding of the polymer ratios impact on the pellets produced.

A focus variation instrument (Contour LS 3D Optical Profiler (Bruker)) was used to assess the surface topography of the pellets using 10 x objective and 2.9 μm lateral resolution. The obtained images were further analysed using the Surfstand™ software (Taylor Hobson, UK, and University of Huddersfield, UK) to obtain 2D and 3D profiles of the surfaces (Ward et al., 2017). The Sq parameter which is defined as the root mean square value of the surface departures from the mean plane within the sampling area was of interest with regards to the influence of the polymer concentration on the pellets produced. This parameter is represented by equation 1:

$$Sq = \sqrt{\frac{1}{A}\iint_A z(x,y)\delta x \delta y} \quad \text{Equation 1}$$

Where:

A = Sampling Area

Z(x,y) = surface departures

2.3.2. Differential scanning calorimetry (DSC)

Thermal studies for the milled samples and their corresponding physical mixture were investigated using the software obtained from Mettler-Toledo, Switzerland. 3-6 mg of the milled and seived samples (Samples A-D) or its physical mixture (Samples PMA-PMD) was placed in a standard aluminium pan with a vented lid and sealed. The crimped pans were

heated from 20 to 250 °C at a scanning rate of 10 °C/min using nitrogen gas to purge the DSC (Mettler-Toledo, Switzerland).

2.3.3. X-ray powder diffraction (XRPD)

Gly, the milled and sieved powder (Samples A-D) and their corresponding physical mixtures (Samples PMA-PMD) were scanned using Bragg–Brentano geometry, over a scattering (Bragg, 2θ) angle range from 5 to 100°, in 0.02° steps at 1.5° min^{-1} using a D2 Phaser diffractometer (Bruker AXS GmbH, Karlsruhe, Germany) (Laity et al., 2015). The XRPD signals were further analysed using Microsoft Excel.

2.4. X-ray microtomography (XμT)

Pellets (as obtained from section 2.2) were imaged by XμT (Nikon XT H 225, Nikon Corp. Tokyo, Japan) using a tungsten target with 75 kV accelerating voltage and 250 μA gun current using a copper filter (thickness 0.125 mm). Pellets were mounted using a double-adhesive tape. A set of projections were collected with over 120 min XμT acquisition. The set of projection images were then reconstructed using CT-Pro and then examined using VG Studio 2.1 software.

2.5. Dynamic contact angle measurement

The sessile drop method (Drop Shape Analysis System, DSA30, Krüss GmbH, Hamburg, Germany) was used to obtain the dynamic contact angle for each formulation (Figure 2) **(contact angle testing was conducted for the milled and sieved samples only – samples A-D)**. This was performed using 1 μL either of deionised water or a FASSIF medium. The liquid was dispensed from a needle to generate a drop and images of the droplet were recorded with a rate of 10 frames per second. The measurements were made at room

temperature in triplicate and the average values and standard deviations were calculated. The initial contact angle was determined from the first ten images (measurement time of 1 s).

2.6. Dissolution analysis

2.6.1 Media preparation:

Biorelevant dissolution media was prepared by dissolving 2.24 g of FASSIF powder for each 1 L of phosphate buffer (pH 7.4). The biorelevant dissolution media was further left under stirring conditions for 2 h. The phosphate buffer was prepared using monobasic potassium phosphate and sodium hydroxide according to the USP pharmacopoeia (Wei and Obenberg, 2006).

2.6.2. Dissolution of the Gly solid dispersions:

A USP I (basket method) apparatus was used for the dissolution testing. 900 mL of dissolution media (section 2.6.1) was filled in a 1L dissolution vessel. The media was heated to 37 ± 0.5 °C. The physical mixtures (PMA-PMD) as well as the milled and sieved powder samples (samples A-D) containing an equivalent of 20 mg Gly content (based on their content uniformity –section 2.2.2) were weighed and then used to fill a size 3 hard gelatine capsule before being transferred to the basket. A rotation speed of 100 rpm was used. The dissolution study was conducted for 2 h. 10 mL of the dissolution media was withdrawn and filtered at the 1, 5, 10, 20, 30, 45, 60, 90 and 120 min predetermined time points for HPLC analysis of Gly content. A preheated biorelevant media was used to replace the 10 mL media taken out after each time point to ensure the constant 900 mL volume. All dissolution studies were conducted in triplicate.

2.6.3. HPLC analysis:

A Shimadzu HPLC system equipped with a C18 column (250 mm x 4.6 mm ID, 4µm, Phenomenex) was used for the Gly analysis. An Isocratic elusion type with a mobile phase of ammonium acetate and acetonitrile (45:55) was used at a flow rate of 1 mL/min. A UV-Vis detector was utilised, and the absorption peak for Gly was investigated at a maximum wavelength of 254 nm. The retention time for Gly was around 2.8 min (Gedeon et al., 2008)

2.6.4. Dissolution parameters

Mean dissolution time (MDT) (Equation 2), defined as the mean time for the drug to dissolve under *in-vitro* dissolution conditions, is a model-independent method and is suitable for dosage forms that have different mechanisms of drug release (Al-Hamidi et al., 2013; Kaialy et al., 2016; Khan, 1975; Mu et al., 2003; Nep et al., 2017)

$$MDT = \frac{\sum_{j=1}^{n} t_j \, \Delta M_j}{\sum_{j=1}^{n} \Delta M_j}, \qquad \text{Equation 2}$$

where j is the sample number, n is the number of dissolution sample times, t_j is the time at midpoint between t_j and t_{j-1} and ΔM_j is the additional amount of drug dissolved between t_j and t_{j-1}.

The dissolution efficiency (DE) (Equation 3) is defined as the area under the dissolution curve up to a certain time *t*, expressed as a percentage of the area of a rectangle described by 100% dissolution in the same time *t* (Asare-Addo et al., 2015; Khan, 1975) was also calculated.

$$DE = \frac{\int_0^t y \times dt}{y_{100} \times t} \times 100, \qquad \text{Equation 3}$$

where *y* is the drug percent dissolved as a function of time *t*.

3. RESULTS AND DISCUSSION

3.1. Solid-state analysis

The thermal analysis of Gly, the milled and sieved products (Samples A-D) and their corresponding physical mixtures (Samples PMA-PMD) are depicted in Figure 3. DSC showed Gly to have a sharp melting point of 175 °C confirming its crystallinity. This was similar to the work published by Cirri et al. (Cirri et al., 2004) who reported Gly to have a sharp melting point at around 175 °C. The physical mixtures of Gly with both Sol and PVP VA64 showed a similar peak at the melting point of Gly but with less intensity. It was also interesting to note that an increase in the polymer content brought about a general reduction in the melting point of Gly. **This behaviour can be attributed to the increased drug polymer interaction with increase polymer content. The increased interactions can cause a melting point depression due to the increase in hydrogen bonding interactions between the drug and polymer (Huang and Dai, 2014; Rim and Runt, 1984).** The physical mixture of Gly with PVP VA64 showed another peak at around 60 °C. This corresponds to the melting point of PEG4000 which was added to the formulations as a plasticiser (Sheskey et al., 2017). The resultant extruded products of Gly:Sol and Gly:PVP VA64 at the two drug loading levels showed no obvious melting point peak for Gly thereby suggesting that Gly had been molecularly dispersed within the polymers used (Figure 3). XRPD confirmed Gly to be completely crystalline in the pure form (Figure 4). Upon inclusion with Sol or PVP VA64 through the HME process, there was a significant reduction in the crystallinity of Gly. It was observed that an increase in the polymer content brought about a further decrease in the crystallinity of Gly. Interestingly, the XRPD data did reveal that samples A-D were not fully amorphous as suggested from the DSC data (Figure 4). Samples A and B however were observed to be more amorphous than C and D suggesting that with the process parameters used for the HME processing, Sol had the greater ability in converting crystalline Gly to its amorphous form which may potentially have implications for

dissolution testing. **The amorphorised regions embedded in the two polymers also suggests that a further manipulation of several processing parameters such as screw speed, screw configuration, feed rate and temperature could impact on the drive towards full amorphorisation.**

3.2. SEM and focus variation analysis

SEM images of the HME pellets, the physical mixtures as well as the milled and sieved fractions of the HME pellets are shown in Figure 5. Gly is crystalline in nature with irregularly shaped particles (Wei et al., 2008). The microstructure of the pellets vary in terms of its overall porosity (further analysed using XμT). Upon magnification, some of the crystalline drug could be seen on the surfaces of some extrudates (highlighted by yellow dashed circles) confirming the XRPD analysis that Gly had not been fully molecularly dispersed into the polymers (Figure 5). This was however not evident on the samples with increased polymer content (Samples B and D).

The images produced from focus variation measurement highlighted significant surface texture across all four extrudes in keeping with SEM (Figure 6). This was indicated by the deep valleys across the x profile (Supplementary material S1). The Sq parameter can be viewed as a measure the vertical scale of the surface. Analysis of the data showed that an increase in polymer content for the extrudates brought about an increase in the Sq value (Sample A, 1:1 Gly:Sol – Sq = 19.83 μm ; Sample B, 1:2 Gly:Sol – Sq = 48.78 μm; Sample C, 1:1 Gly:PVP VA64 – Sq = 26.56 μm; Sample D, 1:2 Gly:PVP VA64 – Sq = 33.58 μm).

3.3. X-ray computed microtomography

The reconstructed XμT cross-sectional images of filaments indicate differences in the microstructure of these filaments confirming the results from SEM (Figure 7). The higher the

electron density of the material, the stronger it absorbs X-rays and hence the intensity values in the XμT images are higher (brighter) (Bentz et al., 2000; Stock, 1999). Sample A (1:1 Gly:Sol) showed a higher porosity (63.72 %) compared to sample B (1:2 Gly:Sol) (57.41 %) suggesting that an increase in the Sol content brought about a decrease in the porosity (converted as a percentage) of the pellets produced. This was true also for samples C (1:1 Gly:PVP VA64) and D (1:2 Gly:PVP VA64). The porosity values for samples C and D were 19.47 % and 14.22 % respectively suggesting also that an increase in polymer content decreases the porosity of pellets produced. The porosity of all the samples were thus in the following order: A > B > C > D. These results suggest that the PVP VA64 makes denser pellets which may well have dissolution consequences.

3.4. Contact angle measurement

Contact angle measurements performed using deionised water initially showed sample A (1:1 Gly:Sol) to have the highest contact angle (90.65 ± 7.06 °). This was followed closely by sample B (1:2 Gly:Sol) with a contact angle of 84.41 ± 2.60 °. Sample C had the lowest contact angle (33.72 ± 1.24 °) followed by sample D with an angle of 41.11 ± 2.33 ° (Figure 8). This suggested samples C and D to be significantly more hydrophilic than samples A and B. Dynamic contact angle measurements for the samples using FASSIF proved surprising and interesting. The contact angles for samples A (1:1 Gly:Sol) and B (1:2 Gly:Sol) could not be obtained as the droplet absorbed very quickly (within a few seconds). As such, the elapsed time for the droplet to be absorbed for these samples were taken into consideration. The mean time for sample A to be absorbed was 1.67 ± 0.50 s, whereas the mean time for sample B to be absorbed was 0.17 ± 0.05 s. This indicates that sample B wets slightly better than sample A. This was in direct contrast to the results from deionised water suggesting that the presence of the various ions in the FASSIF media may have had a solubilising effect on the

samples with an increase in polymer content having a greater effect. Samples C (1:1 Gly:PVP VA64) and D (1:2 Gly:PVP VA64) however had a lower absorption rate compared to samples A and B therefore the dynamic contact angle (Figure 9) could be determined. The data reveals that even though the initial contact angles for samples C and D were similar, sample D wets better than sample C over time. This was also similar to the trend observed for samples A and B where an increase in polymer content seemed to accelerate the ingress of media. In summary, the order of wetting for samples was: B > A > D > C. This change in contact angle order in comparison with deionised water may have implications again for dissolution testing and as such consideration should be made with regards to making appropriate predictions for dissolution based on the media for contact angle testing.

3.5. Dissolution analysis

Results of dissolution testing for capsules filled with the milled and sieved powders are presented in Figure 10. The physical mixtures displayed dissolution profiles similar to that of the pure crystalline drug whereas the HME samples displayed dissolution profiles superior to that of the crystalline drug and the physical mixtures. It was also observed from the dissolution profiles that samples containing Sol had higher dissolution rates in comparison with samples that contained PVP VA64. Furthermore, sample B, which contained 1:2 Gly:Sol, showed a higher dissolution rate in comparison to sample A (1:1 Gly:Sol). This indicates that increasing the level of polymer content increased the dissolution of Gly. A similar trend was observed with sample C and D, with sample D (1:2 Gly:PVP VA64) showing a higher dissolution rate in comparison to sample C (1:1 Gly:PVP VA64). This was confirmed by the MDT, MDR and DE values. Sample A had a DE value of 36.43 %, MDT of 55.40 min and an MDR of 0.51 % min^{-1} while sample B had a DE of 60.53 %, MDT of 29.70 min and MDR of 0.91 % min^{-1}. Sample C had a DE value of 10.17 %, MDT of 66.28 min and MDR of 0.14 % min^{-1} while sample D had a value of DE of 14.44 %, MDT of 65.30 min

and MDR of 0.19 % min^{-1}. It was interesting to note that the dissolution results correlated with the wetting results from the contact angle measurement using the FASSIF media. This indicates that the initial liquid imbibition process as captured by the dynamic contact angle directly affects the dissolution performance. **The authors attribute the dissolution behaviour to the nature of the polymers, its concentration as well as the degree of amorphorisation (it can be observed from figure 4 that Gly is more molecularly dispersed in Sol than in the PVP VA64. This contributed to its increase in wettability as well as dissolution with sample B (higher in amorphous content) being the one with the highest dissolution). This is because the particle sizes of the formulation were controlled (< 250 µm) and further confirmed using laser diffraction (Supplementary material Table S2).**

4. CONCLUSIONS

Solid dispersion of Gly with Sol and PVP VA64 were made at varying concentrations using hot-melt extrusion. The solid dispersions were successfully characterised using a range of techniques. SEM and focus variation analysis showed differences in the microstructure and surface morphology of the samples produced which could be attributed to the level of polymer content present within them. XµT showed an increase in polymer content brought about a decrease in porosity of the hot-melt extruded dispersions with PVP VA64 potentially making denser products which could have its own implications. The static and dynamic contact angle measurement correlated with the dissolution studies using FASSIF media indicating that the initial liquid imbibition process as captured by the dynamic contact angle directly affects the dissolution performance which is of great importance as this techniques could be exploited in predicting dissolution performance.

5. ACKNOWLEDGEMENTS

Maen Al Shafiee acknowledges the EPSRC DTP at the University of Huddersfield for financial support. The authors would like to Dr Paul Bills and Mr Chris Dawson for the generation of the X-ray microtomography images.

6. REFERENCES

Adebisi, A.O., Kaialy, W., Hussain, T., Al-Hamidi, H., Nokhodchi, A., Conway, B.R., Asare-Addo, K., 2016. Solid-state, triboelectrostatic and dissolution characteristics of spray-dried piroxicam-glucosamine solid dispersions. Colloids Surfaces B Biointerfaces 146, 841–851. https://doi.org/10.1016/J.COLSURFB.2016.07.032

Al-Hamidi, H., Asare-Addo, K., Desai, S., Kitson, M., Nokhodchi, A., 2015. The dissolution and solid-state behaviours of coground ibuprofen–glucosamine HCl. Drug Dev. Ind. Pharm. 41, 1682–1692. https://doi.org/10.3109/03639045.2014.991401

Al-Hamidi, H., Edwards, A.A., Douroumis, D., Asare-Addo, K., Nayebi, A.M., Reyhani-Rad, S., Mahmoudi, J., Nokhodchi, A., 2013. Effect of glucosamine HCl on dissolution and solid state behaviours of piroxicam upon milling. Colloids Surfaces B Biointerfaces 103, 189–199. https://doi.org/10.1016/J.COLSURFB.2012.10.023

Al-Hamidi, H., Edwards, A.A., Mohammad, M.A., Nokhodchi, A., 2010a. To enhance dissolution rate of poorly water-soluble drugs: Glucosamine hydrochloride as a potential carrier in solid dispersion formulations. Colloids Surfaces B Biointerfaces 76, 170–178. https://doi.org/10.1016/J.COLSURFB.2009.10.030

Al-Hamidi, H., Edwards, A.A., Mohammad, M.A., Nokhodchi, A., 2010b. Glucosamine HCl as a new carrier for improved dissolution behaviour: Effect of grinding. Colloids Surfaces B Biointerfaces 81, 96–109. https://doi.org/10.1016/J.COLSURFB.2010.06.028

Ali, M. E., & Lamprecht, A. 2017. Spray freeze drying as an alternative technique for lyophilization of polymeric and lipid-based nanoparticles. Int. J. Pharm. 516(1-2), 170-177.

Asare-Addo, K., Šupuk, E., Al-Hamidi, H., Owusu-Ware, S., Nokhodchi, A., Conway, B.R., 2015. Triboelectrification and dissolution property enhancements of solid dispersions. Int. J. Pharm. 485, 306–316. https://doi.org/10.1016/J.IJPHARM.2015.03.013

Asare-Addo, K., Walton, K., Ward, A., Totea, A. M., Taheri, S., Alshafiee, M., ... & Conway, B. R. 2018. Direct imaging of the dissolution of salt forms of a carboxylic acid drug. Int. J. Pharm. 551(1-2), 290-299.

Bentz, D.P., Quenard, D.A., Kunzel, H.M., Baruchel, J., Peyrin, F., Martys, N.S., Garboczi, E.J., 2000. Microstructure and transport properties of porous building materials. II: Three-dimensional X-ray tomographic studies. Mater. Struct. 33, 147–153. https://doi.org/10.1007/BF02479408

Betageri, G.V., Makarla, K.R., 1995. Enhancement of dissolution of glyburide by solid dispersion and lyophilization techniques. Int. J. Pharm. 126, 155–160. https://doi.org/10.1016/0378-5173(95)04114-1

Betageri, G. V., Makarla, K.R., 1996. Characterization of Glyburide-Polyethylene Glycol Solid Dispersions. Drug Dev. Ind. Pharm. 22, 731–734. https://doi.org/10.3109/03639049609063230

Cirri, M., Maestrelli, F., Furlanetto, S., Mura, P., 2004. Solid-state characterization of glyburide-cyclodextrin co-ground products. J. Therm. Anal. Calorim. 77, 413–422. https://doi.org/10.1023/B:JTAN.0000038982.40315.8f

Conway, B.R., Asare-Addo, K., 2016. Solubility Determinations for Pharmaceutical API, in: Webster, G., Bell, R., Jackson, J. (Eds.), Poorly Soluble Drugs. Pan Stanford, New York

Djuris, J., Nikolakakis, I., Ibric, S., Djuric, Z., Kachrimanis, K., 2013. Preparation of carbamazepine–Soluplus® solid dispersions by hot-melt extrusion, and prediction of drug–polymer miscibility by thermodynamic model fitting. Eur. J. Pharm. Biopharm. 84, 228–237. https://doi.org/10.1016/J.EJPB.2012.12.018

Fahr, A., Liu, X., 2007. Drug delivery strategies for poorly water-soluble drugs. Expert Opin. Drug Deliv. 4, 403–416. https://doi.org/10.1517/17425247.4.4.403

Gedeon, C., Kapur, B., Aleksa, K., Koren, G., 2008. A simple and rapid HPLC method for the detection of glyburide in plasma original research communication (analytical). Clin. Biochem. 41, 167–173. https://doi.org/10.1016/J.CLINBIOCHEM.2007.07.025

Guillory, J.K., 2003. Handbook of Pharmaceutical Salts: Properties, Selection, and Use Edited by P. Heinrich Stahl and Camile G. Wermuth. VHCA, Verlag Helvetica Chimica Acta, Zürich, Switzerland, and Wiley-VCH, Weinheim, Germany. 2002. vix + 374 pp. 17.5 × 24.5 cm. ISBN 3-906390-26-8. $130.00. https://doi.org/10.1021/JM030019N

He, Y., Ho, C., Yang, D., Chen, J., Orton, E., 2017. Measurement and Accurate Interpretation of the Solubility of Pharmaceutical Salts. J. Pharm. Sci. 106, 1190–1196. https://doi.org/10.1016/J.XPHS.2017.01.023

Huang, Y., & Dai, W. G. (2014). Fundamental aspects of solid dispersion technology for poorly soluble drugs. *Acta Pharmaceutica Sinica B*, *4*(1), 18-25.

Kaialy, W., Bello, H., Asare-Addo, K., Nokhodchi, A., 2016. Effect of solvent on retarding the release of diltiazem HCl from Polyox-based liquisolid tablets. J. Pharm. Pharmacol. 68, 1396–1402. https://doi.org/10.1111/jphp.12643

Khan, K.A., 1975. The concept of dissolution efficiency. J. Pharm. Pharmacol. 27, 48–49.

Laity, P.R., Asare-Addo, K., Sweeney, F., Šupuk, E., Conway, B.R., 2015. Using small-angle X-ray scattering to investigate the compaction behaviour of a granulated clay. Appl. Clay Sci. 108, 149–164. https://doi.org/10.1016/J.CLAY.2015.02.013

Lian, X., Dong, J., Zhang, J., Teng, Y., Lin, Q., Fu, Y., & Gong, T. 2014. Soluplus® based 9-nitrocamptothecin solid dispersion for peroral administration: preparation, characterization, in vitro and in vivo evaluation. Int. J. Pharm. 477(1-2), 399-407.

Löbenberg, R., Krämer, J., Shah, V.P., Amidon, G.L., Dressman, J.B., 2000. Dissolution Testing as a Prognostic Tool for Oral Drug Absorption: Dissolution Behavior of Glibenclamide. Pharm. Res. 17, 439–444. https://doi.org/10.1023/A:1007529020774

Mu, X., Tobyn, M.J., Staniforth, J.N., 2003. Development and evaluation of bio-dissolution systems capable of detecting the food effect on a polysaccharide-based matrix system. J. Control. Release 93, 309–318. https://doi.org/10.1016/J.JCONREL.2003.08.013

Nagy, Z.K., Balogh, A., Vajna, B., Farkas, A., Patyi, G., Kramarics, Á., Marosi, G., 2012. Comparison of Electrospun and Extruded Soluplus®-Based Solid Dosage Forms of Improved Dissolution. J. Pharm. Sci. 101, 322–332. https://doi.org/10.1002/JPS.22731

Nep, E.I., Mahdi, M.H., Adebisi, A.O., Dawson, C., Walton, K., Bills, P.J., Conway, B.R., Smith, A.M., Asare-Addo, K., 2017. The influence of hydroalcoholic media on the performance of Grewia polysaccharide in sustained release tablets. Int. J. Pharm. 532, 352–364. https://doi.org/10.1016/J.IJPHARM.2017.09.022

Newman, A., Nagapudi, K., Wenslow, R., 2015. Amorphous solid dispersions: a robust platform to address bioavailability challenges. Ther. Deliv. 6, 247–261. https://doi.org/10.4155/tde.14.101

Nokhodchi, A., Al-Hamidi, H., Adebisi, A.O., Asare-Addo, K., Maniruzzaman, M., 2017. The use of various organic solvents to tailor the properties of ibuprofen–glucosamine HCl solid dispersions. Chem. Eng. Res. Des. 117, 509–519. https://doi.org/10.1016/J.CHERD.2016.11.004

Pas, T., Vergauwen, B., & Van den Mooter, G. (2018). Exploring the feasibility of the use of biopolymers as a carrier in the formulation of amorphous solid dispersions–Part I: Gelatin. Int. J. Pharm. 535(1-2), 47-58.

Paudel, A., Worku, Z.A., Meeus, J., Guns, S., Van den Mooter, G., 2013. Manufacturing of solid dispersions of poorly water soluble drugs by spray drying: Formulation and process considerations. Int. J. Pharm. 453, 253–284. https://doi.org/10.1016/J.IJPHARM.2012.07.015

Ponnammal, P., Kanaujia, P., Yani, Y., Ng, W., Tan, R., Ponnammal, P., Kanaujia, P., Yani, Y., Ng, W.K., Tan, R.B.H., 2018. Orally Disintegrating Tablets Containing Melt Extruded Amorphous Solid Dispersion of Tacrolimus for Dissolution Enhancement. Pharmaceutics 10, 35. https://doi.org/10.3390/pharmaceutics10010035

Rabinow, B.E., 2004. Nanosuspensions in drug delivery. Nat. Rev. Drug Discov. 3, 785–796. https://doi.org/10.1038/nrd1494

Ramirez, M., David, S.E., Schwalbe, C.H., Asare-Addo, K., Conway, B.R., Timmins, P., 2017. Crystal Packing Arrangement, Chain Conformation, and Physicochemical

Properties of Gemfibrozil Amine Salts. Cryst. Growth Des. 17, 3743–3750. https://doi.org/10.1021/acs.cgd.7b00352

Rim, P. B., & Runt, J. P. (1984). Melting point depression in crystalline/compatible polymer blends. *Macromolecules*, *17*(8), 1520-1526.

Savjani, K.T., Gajjar, A.K., Savjani, J.K., 2012. Drug Solubility: Importance and Enhancement Techniques. ISRN Pharm. 2012, 1–10. https://doi.org/10.5402/2012/195727

Sawicki, E., Beijnen, J. H., Schellens, J. H., & Nuijen, B. 2016. Pharmaceutical development of an oral tablet formulation containing a spray dried amorphous solid dispersion of docetaxel or paclitaxel. Int. J. Pharm. 511(2), 765-773.

Serajuddin, A.T.M., 1999. Solid dispersion of poorly water- soluble drugs: Early promises, subsequent problems, and recent breakthroughs. J. Pharm. Sci. 88, 1058–1066. https://doi.org/10.1021/js980403l

Sheskey, P.J., Cook, W.G., Cable, C.G., 2017. Handbook of pharmaceutical excipients, 8th Revise. ed. Pharmaceutical Press.

Solanki, N.G., Tahsin, M., Shah, A. V., Serajuddin, A.T.M., 2018. Formulation of 3D Printed Tablet for Rapid Drug Release by Fused Deposition Modeling: Screening Polymers for Drug Release, Drug-Polymer Miscibility and Printability. J. Pharm. Sci. 107, 390–401. https://doi.org/10.1016/J.XPHS.2017.10.021

Stahl, P.H., Wermuth, C.G., International Union of Pure and Applied Chemistry., 2008. Handbook of pharmaceutical salts : properties, selection, and use, Chemistry International.

Stock, S.R., 1999. X-ray microtomography of materials. Int. Mater. Rev. 44, 141–164. https://doi.org/10.1179/095066099101528261

Šupuk, E., Ghori, M.U., Asare-Addo, K., Laity, P.R., Panchmatia, P.M., Conway, B.R., 2013. The influence of salt formation on electrostatic and compression properties of flurbiprofen salts. Int. J. Pharm. 458, 118–127. https://doi.org/10.1016/J.IJPHARM.2013.10.004

Van den Mooter, G., 2012. The use of amorphous solid dispersions: A formulation strategy to overcome poor solubility and dissolution rate. Drug Discov. Today Technol. 9, e79–e85. https://doi.org/10.1016/J.DDTEC.2011.10.002

Vasconcelos, T., Sarmento, B., Costa, P., 2007. Solid dispersions as strategy to improve oral bioavailability of poor water soluble drugs. Drug Discov. Today 12, 1068–1075. https://doi.org/10.1016/J.DRUDIS.2007.09.005

Wei, H., Dalton, C., Di Maso, M., Kanfer, I., Löbenberg, R., 2008. Physicochemical characterization of five glyburide powders: A BCS based approach to predict oral absorption. Eur. J. Pharm. Biopharm. 69, 1046–1056. https://doi.org/10.1016/J.EJPB.2008.01.026

Wei, H., Löbenberg, R., 2006. Biorelevant dissolution media as a predictive tool for glyburide a class II drug. Eur. J. Pharm. Sci. 29, 45–52. https://doi.org/10.1016/J.EJPS.2006.05.004

Wei, H., Obenberg, R., 2006. Biorelevant dissolution media as a predictive tool for glyburide a class II drug. https://doi.org/10.1016/j.ejps.2006.05.004

Figure captions

Figure 1. Structure of Glyburide, Soluplus® and Kollidon® PVP VA64 used in the manufacture of pellets from the hot-melt extrusion process for the formulations (Samples A-D)

Figure 2. Contact angle testing instrumentation used in the study to determine the wettability and initial liquid imbibition of the solid dispersions produced

Figure 3. DSC thermograms of (A) crystalline Gly, the physical mixtures of (B) 1:1 Gly:Sol, (C) 1:2 Gly:Sol, (D) 1:1 Gly:PVP VA64, (E) 1:2 Gly:PVP VA64, and the hot-melt extruded samples of (F) 1:1 Gly:Sol, (G) 1:2 Gly:Sol, (H)1:1 Gly:PVP VA64 , (I) 1:2 Gly:PVP VA64.

Figure 4. XRD of (A) crystalline Gly, the physical mixtures of (B) 1:1 Gly: Sol , (C) 1:2 Gly: Sol, (D) 1:1 Gly:PVP VA64, (E) 1:2 Gly:PVP VA64, and the hot-melt extruded samples of (F) 1:1 Gly:Sol, (G) 1:2 Gly:Sol, (H)1:1 Gly:PVP VA64 , (I) 1:2 Gly:PVP VA64.

Figure 5. SEM images of Gly, (A) HME extrudate pellets of 1:1 Gly:Sol (sample A) formulation, (A1) physical mixture of 1:1 Gly:Sol, (A2) 1:1 Gly:Sol (milled and sieved sample from HME extrude pellets of A), (B) HME extrudate pellets of 1:2 Gly:Sol (sample B) formulation, (B1) physical mixture of 1:2 Gly:Sol, (B2) 1:2 Gly:Sol (milled and sieved sample from HME extrude pellets of B), (C) HME extrudate pellets of 1:1 Gly:PVP VA64 (sample C) formulation (C1) physical mixture of 1:1 Gly:PVP VA64 (C2) 1:1 Gly:PVP VA64 (milled and sieved sample from HME extrude pellets of C), (D) HME extrudate of 1:2 Gly:PVP VA64 (sample D) formulation, (D1) physical mixture of 1:2 Gly:PVP VA64 (D2) 1:2 Gly:PVP VA64 (milled and sieved sample from HME extrude pellets of D).

Figure 6. Focus variation images of (A) HME extrudate pellet of 1:1 Gly:Sol (sample A) formulation, (B) HME extrudate pellet of 1:2 Gly:Sol (sample B) formulation, (C) HME extrudate pellet of 1:1 Gly:PVP VA64 (sample C) formulation, (D) HME extrudate pellet of 1:2 Gly:PVP VA64 (sample D) formulation.

Figure 7. XμT of sagittal and diametric images of formulated HME extrudate pellet (A) HME extrudate pellet of 1:1 Gly:Sol (sample A), (B) HME extrudate pellet of 1:2 Gly:Sol (Sample B), (C) HME extrudate pellet of 1:1 Gly:PVP VA64 (sample C), (D) HME extrudate pellet of 1:2 Gly:PVP VA64 (sample D).

Note: Colour code for density histogram: Figure 7A-D, red colour is Gly, green and blue colour are polymer (Sol or PVP VA64) and black represents the pores

Figure 8. Contact angle testing of (A) 1:1 Gly:Sol (sample A), (B) 1:2 Gly:Sol (Sample B), (C) 1:1 Gly:PVP VA64 (Sample C), (D) 1:2 Gly:PVP VA64 (Sample D) and (E) a plot of all the contact angle degrees of samples A-D for comparison.

Figure 9. Dynamic contact angle measurement of samples C (1:1 Gly:PVP VA64) and D (1:2 Gly:PVP VA64) using FASSIF as the media

Figure 10. Dissolution profiles for 1:1 Gly:Sol (sample A), 1:2 Gly:Sol (Sample B), 1:1 Gly:PVP VA64 (Sample C), 1:2 Gly:PVP VA64 (Sample D) together with their corresponding physical mixtures PMA-PMD over 120 min

Figures

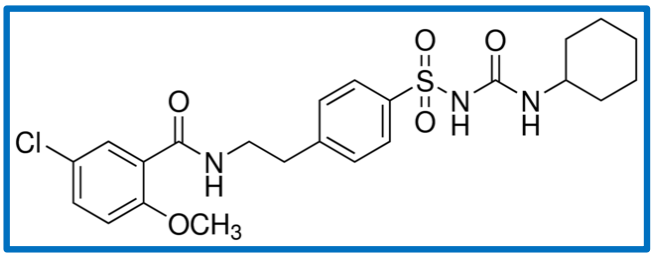

Glyburide

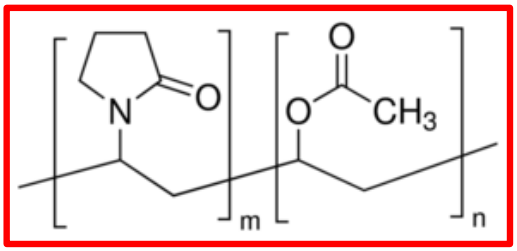

Kollidon® PVP VA 64

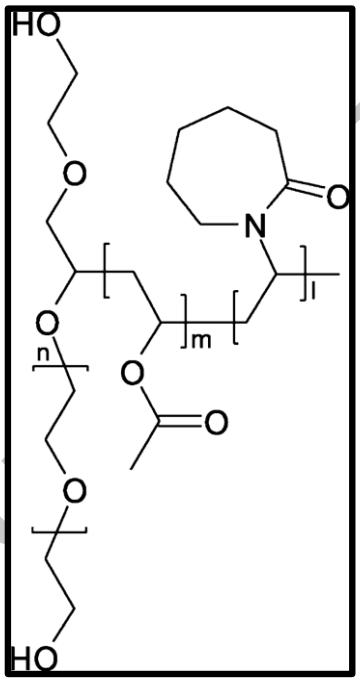

Soluplus®

Figure 1.

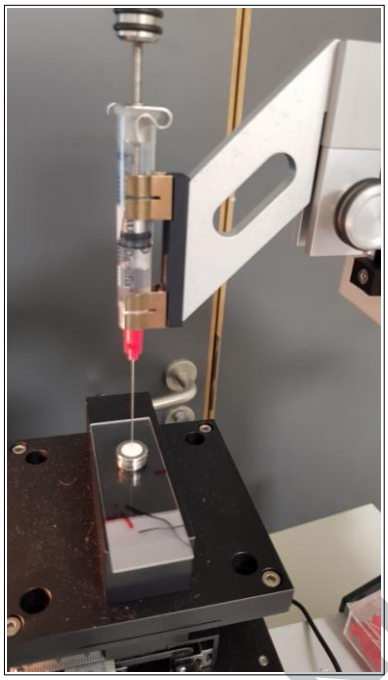

Figure 2.

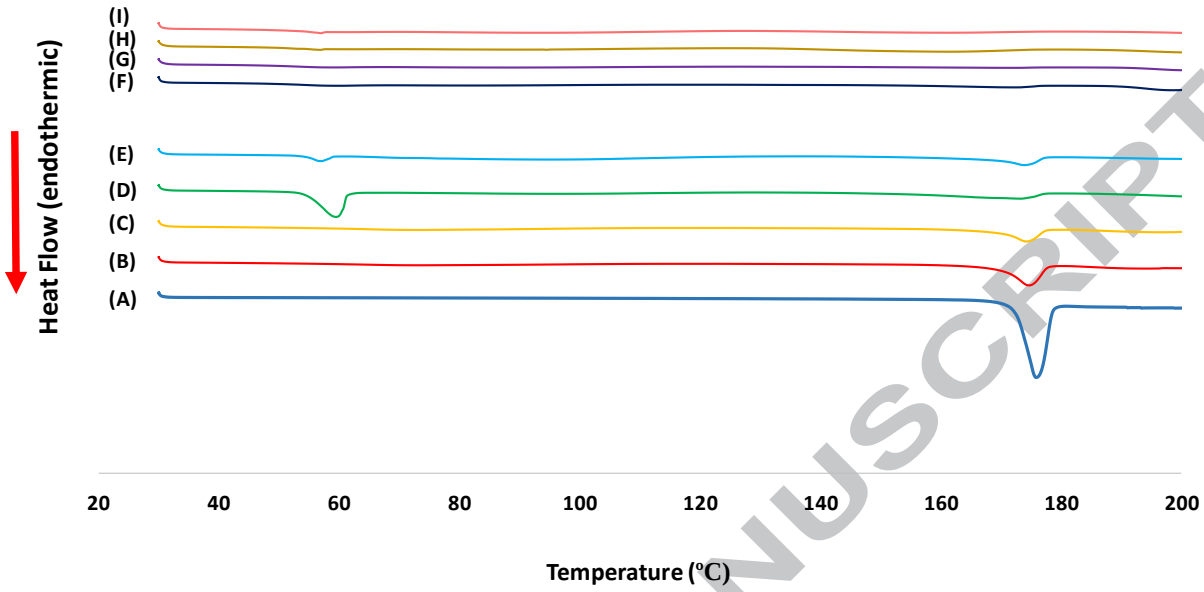

Figure 3.

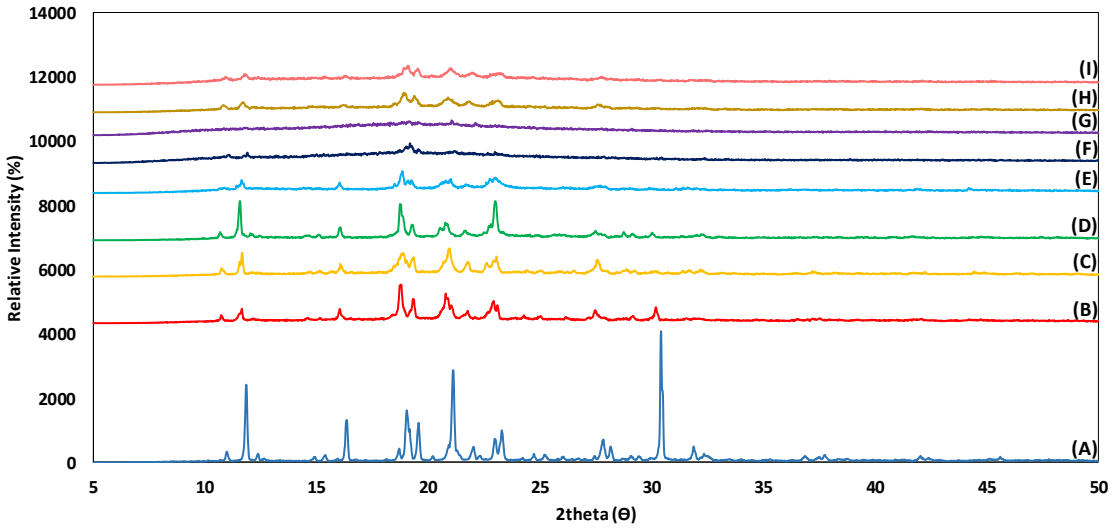

Figure 4.

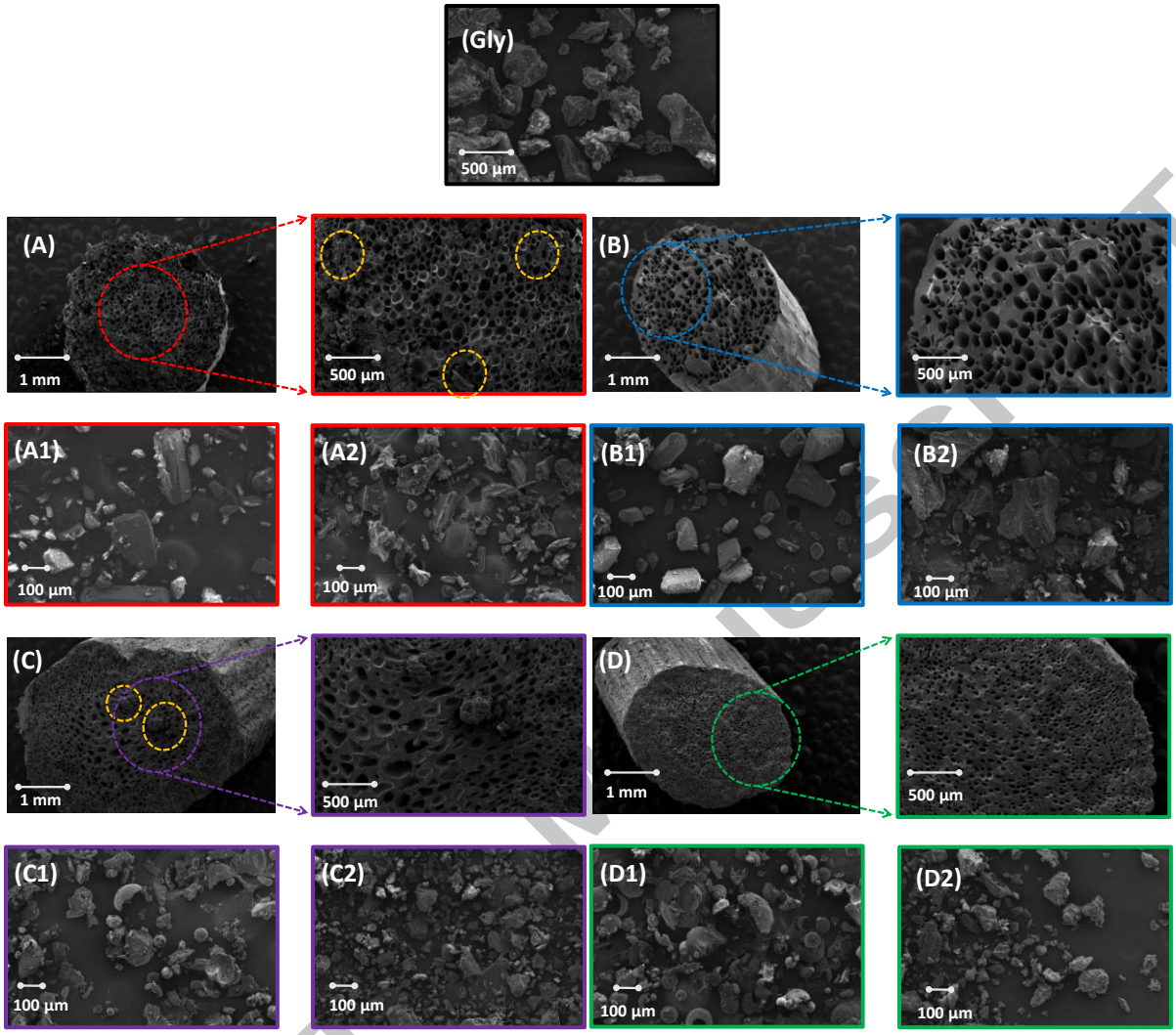

Figure 5.

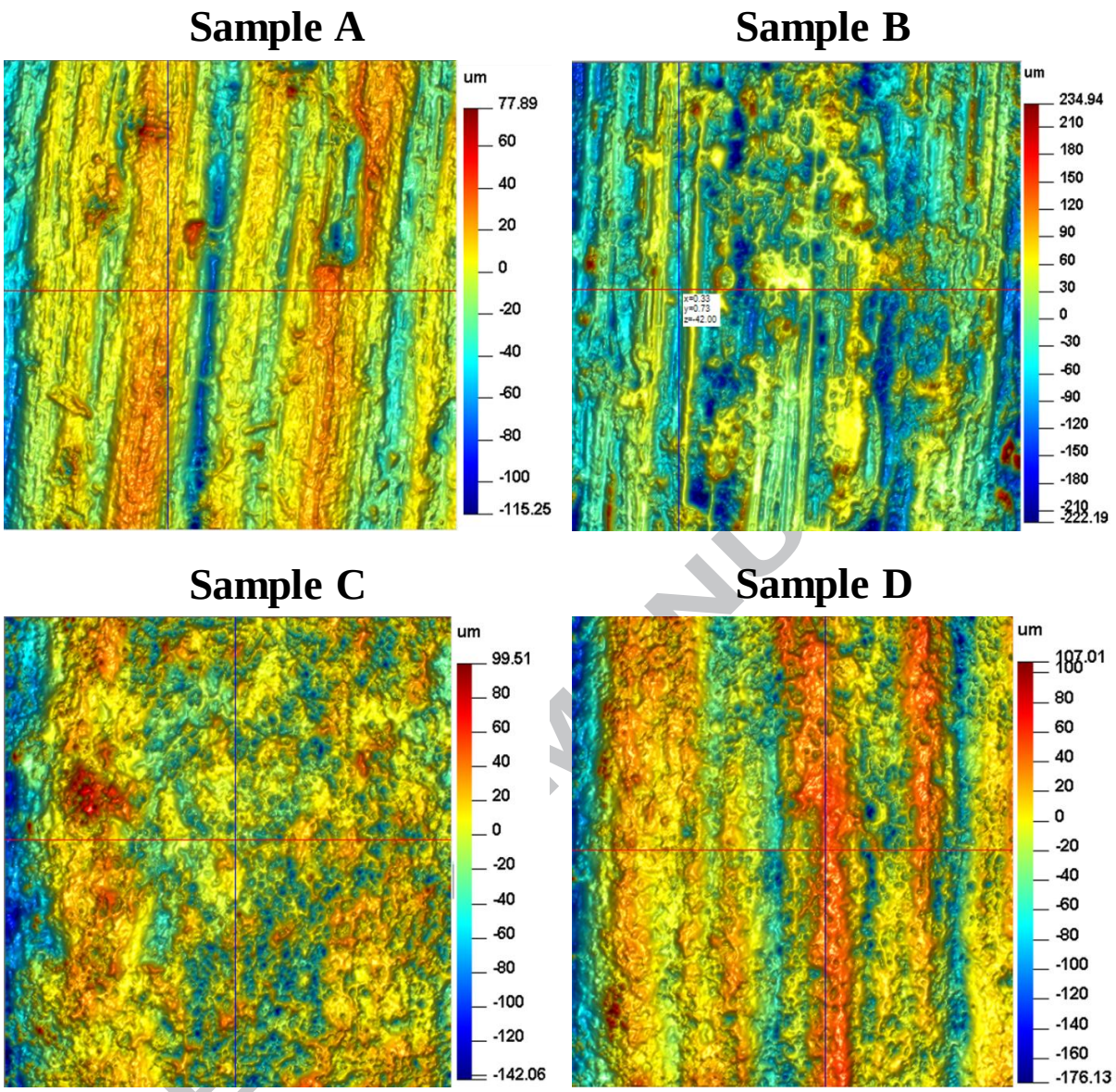

Figure 6.

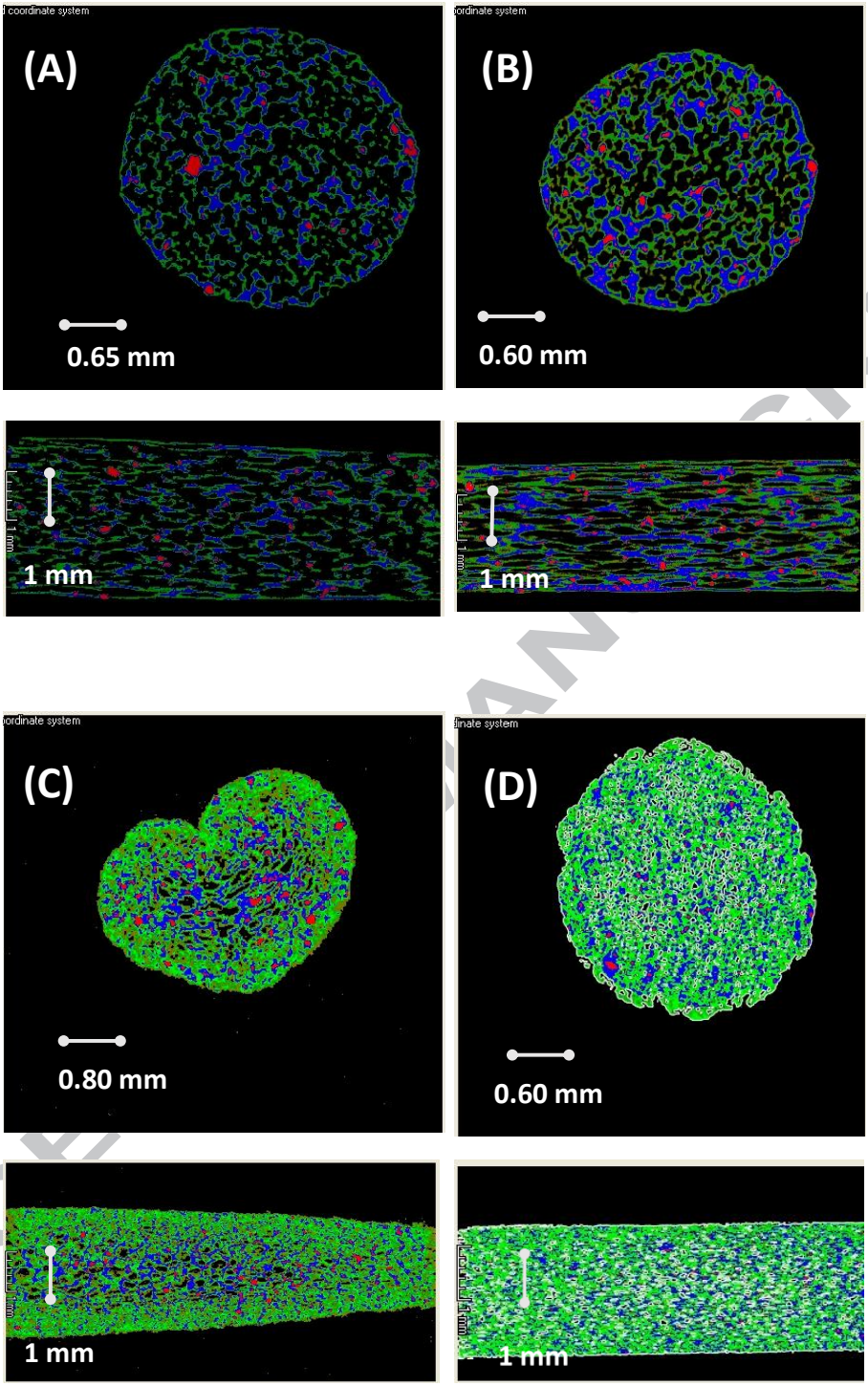

Figure 7.

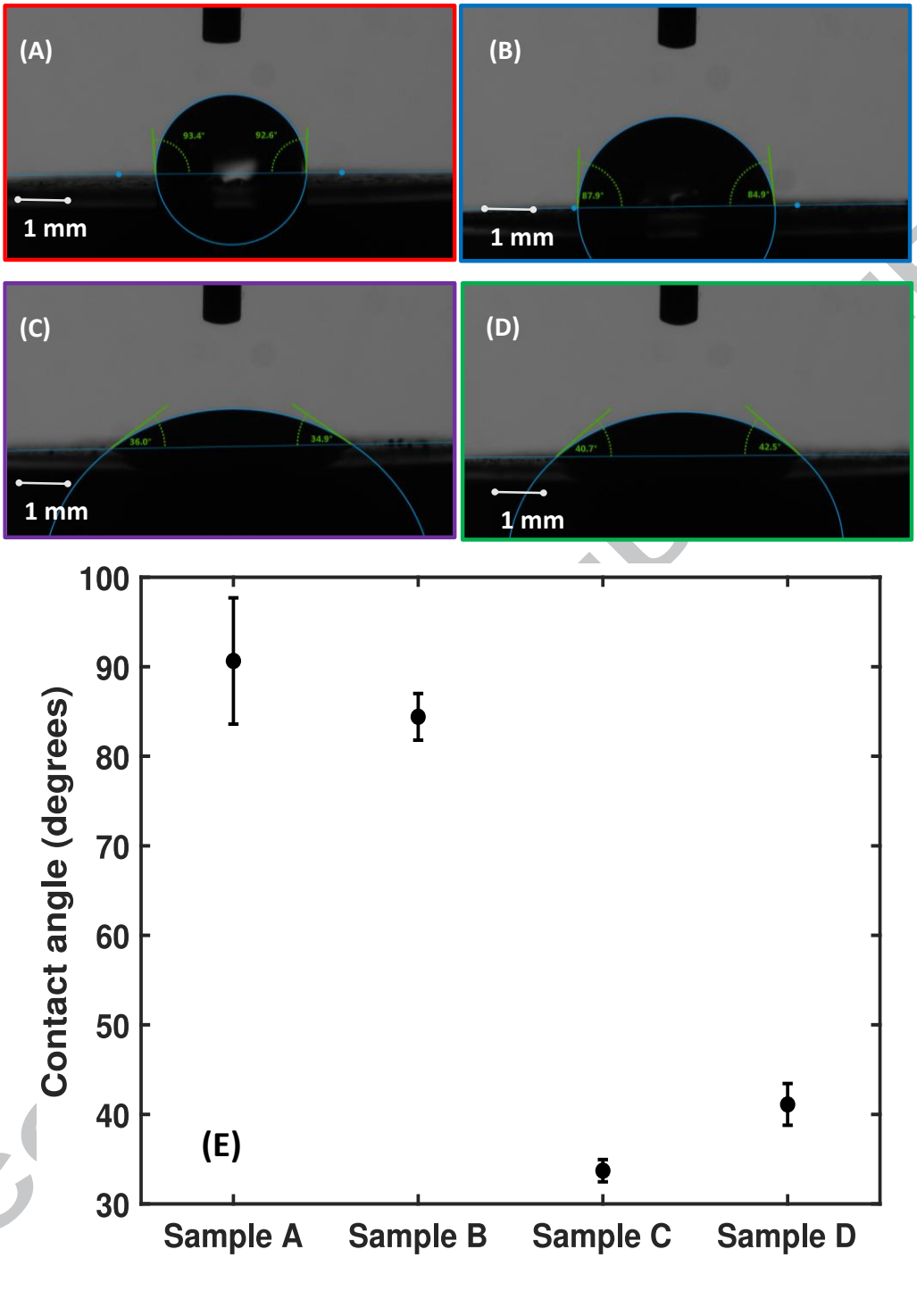
(A)
93.4°
92.6°
1 mm
(B)
87.9°
84.9°
1 mm
(C)
36.0°
34.9°
1 mm
(D)
40.7°
42.5°
1 mm
Contact angle (degrees)
100
90
80
70
60
50
40
30
(E)
Sample A
Sample B
Sample C
Sample D

Figure 8.

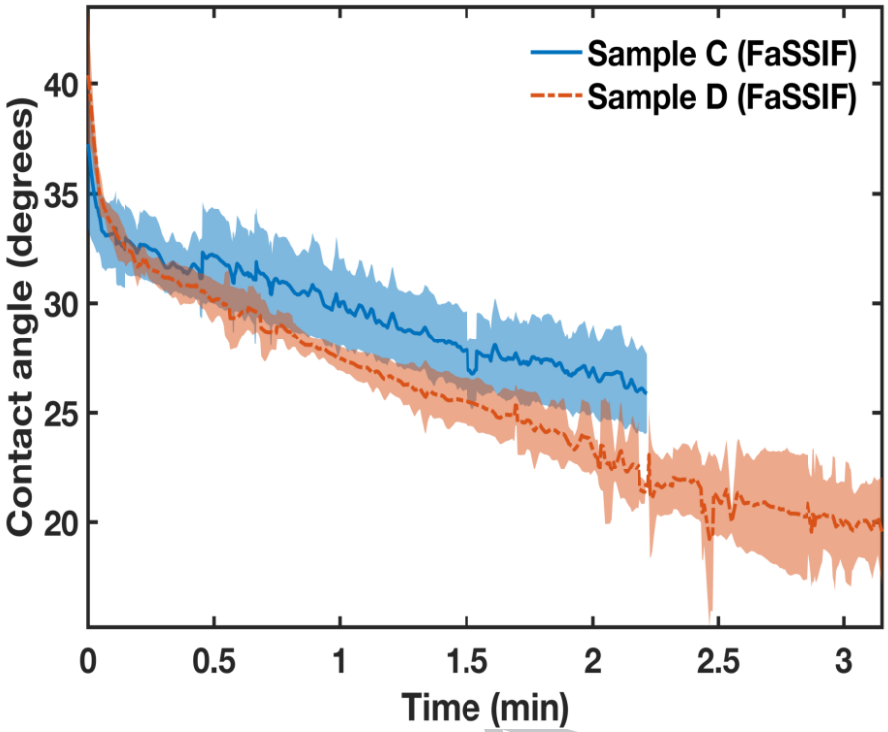

Figure 9.

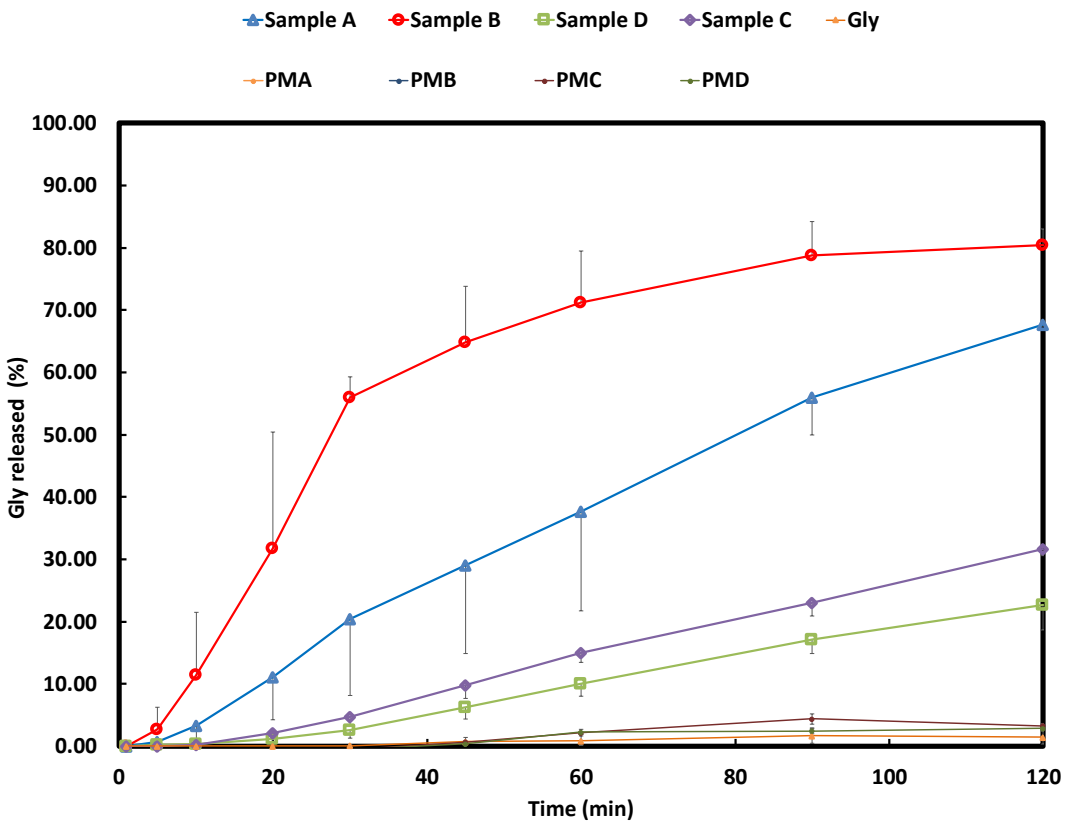

Figure 10.

Highlights

1. Solid dispersions of glyburide made by hot-melt extrusion

2. SEM and focus variation analysis showed microstructure and surface morphology was significantly different between samples

3. XμT showed that an increase in polymer content brought about a decrease in porosity

4. Static and dynamic contact angle measurement correlated with the dissolution studies using FASSIF media

5. Results show the initial liquid imbibition process captured by the dynamic contact angle directly affects the dissolution performance

Graphical Abstract

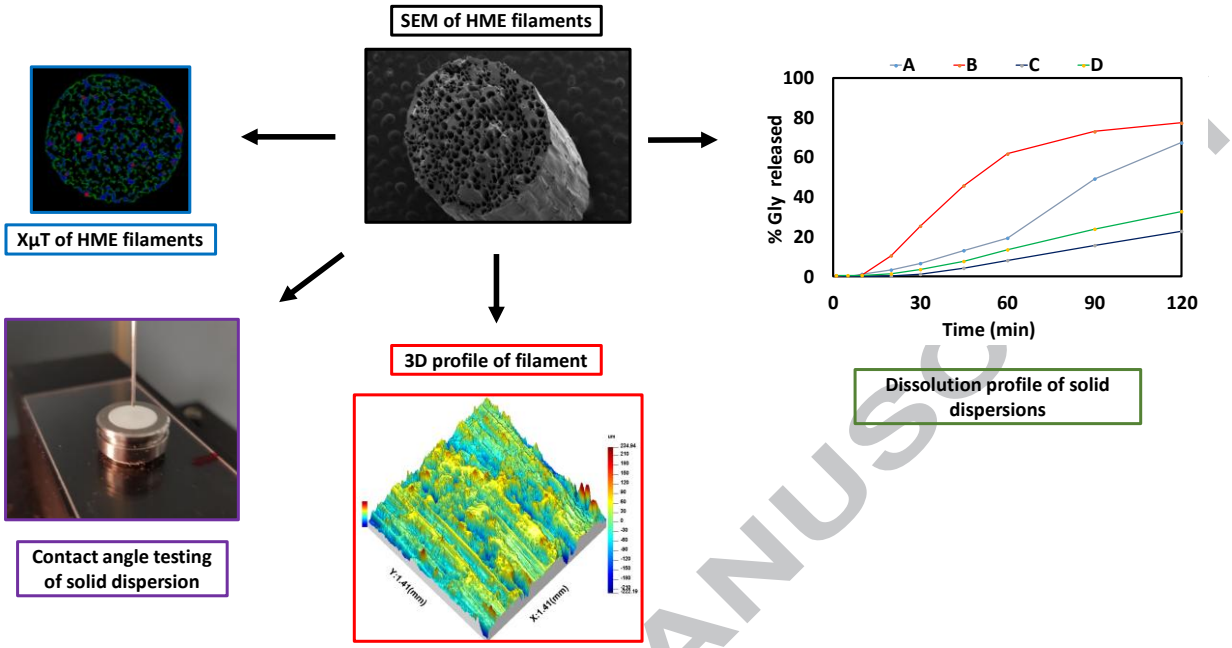

The authors declare no conflict of interest in this work